Dynamic Materials

Deutsche Ausgabe: DOI: 10.1002/ange.201604868
Internationale Ausgabe: DOI: 10.1002/anie.201604868

Controlling the Localization of Liquid Droplets in Polymer Matrices by Evaporative Lithography

Huaixia Zhao, Jiajia Xu, Guangyin Jing, Lizbeth Ofelia Prieto-López, Xu Deng, and Jiaxi Cui**

Dedicated to Professor Eduard Arzt on the occasion of his 60th birthday

Abstract: *Localized inclusions of liquids provide solid materials with many functions, such as self-healing, secretion, and tunable mechanical properties, in a spatially controlled mode. However, a strategy to control the distribution of liquid droplets in solid matrices directly obtained from a homogeneous solution has not been reported thus far. Herein, we describe an approach to selectively localize liquid droplets in a supramolecular gel directly obtained from its solution by using evaporative lithography. In this process, the formation of droplet-embedded domains occurs in regions of free evaporation where the non-volatile liquid is concentrated and undergoes a phase separation to create liquid droplets prior to gelation, while a homogeneous gel matrix is formed in the regions of hindered evaporation. The different regions of a coating with droplet embedment patterns display different secretion abilities, enabling the control of the directional movement of water droplets.*

The insertion of a liquid into a solid matrix in the form of discrete droplets constitutes a promising approach to regulate material properties.[1] It can provide a mechanism for the self-recovery of surface damage,[2] to mediate optical properties,[3] to maintain surface wettability and slipperiness,[4] and to tune the material strength, for example.[5] Fundamental to these functions is the liquid storage within the solid matrix. Unlike solid compositions, which are easily assembled and localized, liquids are mobile and intrinsically cohesive. They are often packaged into solid-like particles through molecular self-assembly or microfluidic emulsification before integration into solid matrices.[6] These processes challenge the direct localization of liquid inclusions in a solid matrix produced from a homogeneous solution and then make precise/targeted delivery, fine mediation of the surface properties, and the control of water movement on the surface difficult.[7] Herein, we describe a method to use evaporative lithography to control the localized incorporation of liquid droplets into dynamic polymer matrices. Evaporative lithography is a novel technique to control particle migration during the drying of a liquid phase. It is based on the mediation of solvent evaporation with masks,[8] and inspired by the coffee ring phenomenon, which refers to the drying of a suspension droplet, in which heterogeneous evaporation rates cause an internal flow and result in the localized deposition of particles.[9]

To create polymer matrices with embedded liquid droplets by evaporative lithography, the starting system should contain three components: a polymer able to form a cross-linked matrix after solvent evaporation, a nonvolatile liquid to be encapsulated, and a volatile solvent that can dissolve both the polymer precursor and the liquid. The nonvolatile liquid should have low solubility in the resulting polymer matrix so that the excess liquid can undergo phase separation and form liquid droplets.[4b] Copolymers of urea and polydimethylsiloxane (uPDMS), which can entrap oil droplets (i.e., silicone oil) by reversible formation of hydrogen bonds between urea units when gelled from a solution of volatile tetrahydrofuran (THF),[4b] were selected as the starting polymer precursor. Various copolymers uPDMS-R with different terminal groups (R = Me, NH_2, or NCO) were synthesized to explore the influence of different units on the polymer matrices (Figure 1 a). These polymers have a similar molecular weight but different stiffness (Young's modulus: uPDMS-NH_2 > uPDMS-NCO > uPDMS-Me; see the Supporting Information, Figure S1 and Table S1). All uPDMS polymers can be dissolved in THF together with silicone oil (viscosity: 10 cSt) to produce homogeneous starting solutions.

We prepared the polymer coatings by placing the starting solution on a flat substrate and then letting it dry while covered with a mask above the liquid surface at a distance d (Figure 1). This mask provides a way of regulating the rate of THF evaporation from the coating. In the uncovered regions, THF evaporated and escaped at a significantly higher rate than in the covered regions. This fast evaporation leads to an increase in the concentrations of the uPDMS and silicone oil in the uncovered regions, creating a concentration-gradient-driven surface tension force along the interface between air and solution. As THF has a higher surface tension than

[*] Dr. H. Zhao, Prof. X. Deng, Dr. J. Cui
Institute of Fundamental and Frontier Sciences
University of Electronic Science and Technology of China
No. 4, Section 2, North Jianshe Road, Chengdu, Sichuan (China)
E-mail: dengxu@uestc.edu.cn
jiaxi.cui@leibniz-inm.de
Dr. H. Zhao, J. Xu, Dr. L. O. Prieto-López, Dr. J. Cui
INM-Leibniz Institute for New Materials
Campus D2 2, 66123 Saarbrücken (Germany)
Prof. G. Jing
National Key Laboratory and Incubation Base of Photoelectric Technology and Functional Materials and School of Physics
Northwest University, 710069 (China)
and
PMMH, CNRS-UMR 7636, ESPCI-ParisTech
10 Rue Vauquelin, 75005 Paris (France)
Supporting information and the ORCID identification numbers for the authors of this article can be found under http://dx.doi.org/10.1002/anie.201604868.

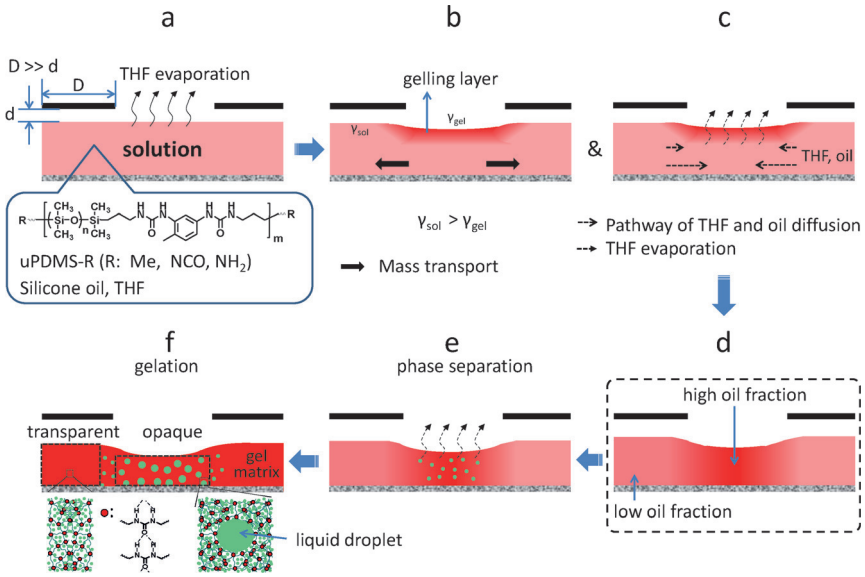

Figure 1. Controlling the localization of liquid droplets in a gel matrix through evaporative lithography. a) A homogeneous solution consisting of the cross-linkable polymer uPDMS, silicone oil, and volatile THF is coated onto a flat substrate with a mask. b) THF evaporation from the uncovered areas induces asymmetric surface tension, which leads to mass transport in the solution from the uncovered to the covered regions. c) THF diffuses from the covered regions to the uncovered ones, alongside silicone oil. d) Asymmetric distribution of the silicone oil fraction. e) Phase separation of excess silicone oil in uncovered regions leads to the formation of pure silicone droplets. f) Gelation to form a patterned coating.

silicone oil and uPDMS, the surface tension gradient drives the so-called Marangoni flow, carrying polymer and silicone oil from the low-surface-tension regions (uncovered regions) to the higher-surface-tension regions (covered region; Figure 1b, see also Section S4). Simultaneously, faster THF evaporation in the uncovered regions produces a concentration gradient so that THF diffuses from the covered to the uncovered regions (Figure 1c). THF transport was expected to be accompanied by the transfer of silicone oil molecules owing to the good affinity of THF to silicone oil. On the other hand, uPDMS is difficult to transport with THF molecules owing to its cross-linkable nature and higher molecular weight. Instead, uPDMS acted as a porous matrix for the diffusion of small liquid molecules. The selective evaporation induced an asymmetric distribution of the silicone oil composition (Figure 1d). With further evaporation, excess silicone oil underwent phase separation to create pure liquid droplets, which was followed by the gelation of uPDMS to form a solid matrix (Figure 1e,f).

Polymer films obtained by evaporative lithography display patterned optical properties (Figure 2a). The covered regions are transparent whereas the uncovered regions are opaque (Figure 2b). The transparent regions are slightly thicker than the opaque ones as observed in the cross-section image (Figure 2c). This pattern is opposite to the colloidal pattern obtained by evaporative lithography in which colloid particles accumulate and form a plateau in the areas of higher solvent evaporation owing to convective nanoparticle flow.[10] In our case, the increased thickness in the covered regions suggests that a mass transport from uncovered regions takes places, which was mainly attributed to the concentration-driven surface tension gradient induced by selective evaporation[11] (Figure S2). THF (27 $mN\,m^{-1}$) has a higher surface tension than silicone oil (21 $mN\,m^{-1}$) and uPDMS (similar to that of silicone elastomer, estimated by the water contact angle; see Figure S3). Therefore, the surface tension of the mixture decreases in the THF-depleted region owing to faster evaporation (Figure S4). To support this idea of surface-tension-driven movement, we placed droplets of various mixtures of THF, silicone oil, and uPDMS on flat substrates and covered them partially, thus creating asymmetric surface tension, and their movement was recorded (Movies S1 and S2). As expected, we observed that each droplet deformed and moved towards the covered area.

Confocal microscopy was used to probe the formation and localization of the liquid droplets in the uPDMS matrices. To enable imaging, the fluorescence marker perylenediimide (PDI) was conjugated to the silicone oil (see Figure S5). In the opaque region, discrete droplets of pure silicone oil were observed as bright spots,[4b] which were uniformly dispersed throughout a relatively dark continuous matrix of polymer and liquid (Figure 2d). In the transparent region, only a homogeneous polymer–liquid matrix was observed without liquid droplets. A transition zone could be observed between the opaque and the transparent regions with a clear size and density gradient for the liquid droplets. The redistribution of the compositions that is induced by regional evaporation was further confirmed by UV/Vis and FTIR spectroscopy (Figure 2e,f). Silicone oil was dyed with PDI, such that the stronger PDI absorption in the UV/Vis spectrum of the material in the uncovered regions represented a higher concentration of silicone oil (by a factor of 1.38).[12] The reduced amount of uPDMS in this region was further confirmed by the weaker carboxyl absorption in the FTIR spectrum.

We also compared the liquid droplets formed during drying with and without masking (Figure 3a). The liquid droplets in the coating covered with a mask were bigger than those formed in the absence of a mask. The evaporation of solvent during the self-forming process of liquid droplets in current material systems induces both phase separation and gelation. The droplets are produced in the process of phase separation and then fixed during gelation.[4b] A suitable time window between phase separation and gelation allows the droplets to fuse to reduce the interface energy. In evaporative lithography, the supplement of THF from the covered region amplifies this time window, leaving more time for the droplets to fuse. This hypothesis was also supported by the lower density and higher dispersity of the droplets observed in the masked sample. On the other hand, localized silicone oil enrichment also contributed to the increase in droplet size.

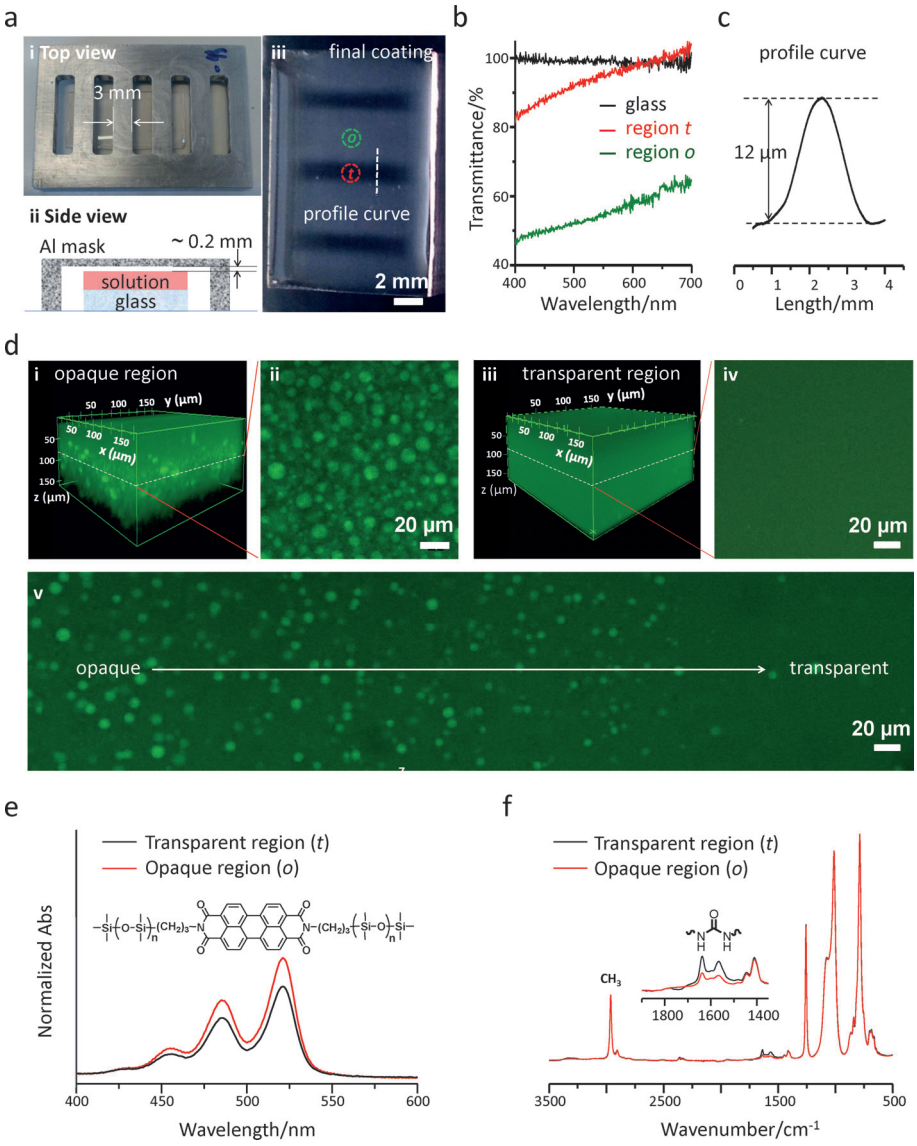

Figure 2. Structural characterization of the gel coatings containing localized droplets. a) Patterned coating obtained by evaporative lithography. i, ii) Evaporative lithography setup. iii) Optical image of the coating obtained. Marks on the image show the positions used for collecting data. b) The transmittance curves of different regions marked on the picture (a, iii) and a glass control. c) The profile curve obtained from the marked line in (a, iii). d) Confocal fluorescence images obtained from different regions, using PDI-conjugated silicone oil to visualize the liquid. i, ii) 3D and 2D view of the opaque (uncovered) region. iii, iv) 3D and 2D view of the transparent (covered) region. v) Overall image. e) UV/Vis and f) FTIR spectra of the samples for the different regions. The coatings were prepared from a solution of uPDMS-Me (30 wt%) in THF with a silicone oil loading of 160 wt% (oil/uPDMS), and have a thickness of 320 ± 20 µm. The plot diameter used for the transmittance measurement is 2 mm.

This enrichment effect could be used to create liquid droplets from an unsaturated solution. For example, the saturation loading of uPDMS-Me with silicone oil was 98 wt% (oil/uPDMS, estimated by the swelling of uPDMS-Me in silicone oil). Its THF solution with a silicone oil loading of 90 wt% formed a transparent film in the absence of a mask (Figure 3b). However, when this unsaturated solution was used in evaporative lithography, the silicone oil was concentrated in the uncovered regions, creating an oversaturated state and thus generating liquid droplets. Without selective evaporation, droplets are formed homogeneously throughout the depth of the film.[4b] To evaluate the influence of evaporative lithography on the distribution of the liquid droplets in the cross-section, we prepared a thicker sample in a sealed chamber with THF vapor. The droplets in the resulting coating were bigger than those formed under normal conditions but did not show a distribution gradient within the whole depth profile scale (Figure S6).

We further investigated the localization effect of evaporative lithography on different polymer systems. We first tested the formation of liquid droplets in uPDMS with different terminal groups. Surprisingly, the terminal groups had a remarkable influence on the kinetics of gelation: Both uPDMS-NCO and uPDMS-Me gelled slowly to produce big liquid droplets, whereas the timescale for uPDMS-NH_2 gelation was on the same order as that for phase separation and offered less time for the droplets to fuse (Figure 3c, Table S1). This effect was attributed to the stronger cross-linking of uPDMS-NH_2 (Table S1) in which the amino terminal groups, which are involved in cross-linking, triggered faster gelation. All three polymers were able to produce patterned droplet-embedded coatings by evaporative lithography. Although the droplets in the uPDMS-NH_2 system were slightly bigger than those in the control, we did not observe a significant decrease in the density of droplets (Figure 3d). This finding suggests that in the uPDMS-NH_2 system, the addition of THF did not significantly widen the time window between the phase separation and the gelation to allow for droplet fusion. From these results, we can conclude that evaporative lithography has a certain influence on the kinetics of phase separation and gelation but does not change their intrinsic order.

The release of stored liquids from matrices is crucial to recover many material functions.[2,4] The silicone oil droplets stored in our dynamic uPDMS matrices can secrete oil to the surface or damaged regions to maintain the interfacial slipperiness.[4b,13] The localization of silicone oil droplets was

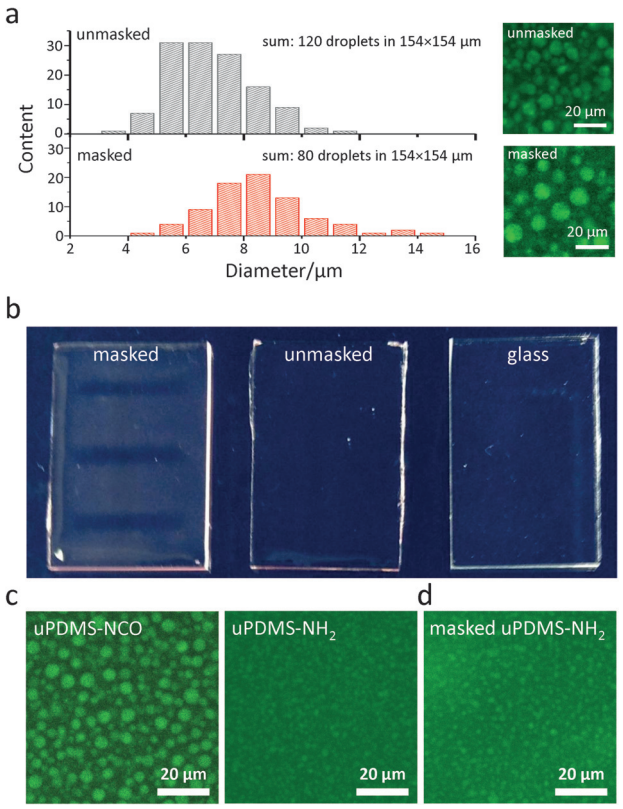

Figure 3. Comparison of the gel coatings obtained with and without a mask. a) Comparison of the droplets formed in masked and unmasked samples made from a THF solution of uPDMS-Me with a silicone oil loading of 160 wt% (oil/uPDMS). The number of droplets was estimated from 2D images. b) Optical images of gel coatings with (left) and without (middle) a mask obtained from a THF solution of uPDMS-Me with a silicone oil loading of 90 wt%. A glass control is shown for comparison (right). Confocal images of gel coatings made from uPDMS-NCO and uPDMS-NH_2 without a mask (c) and from uPDMS-NH_2 with a mask (d). The silicon oil loading of the samples in (c) and (d) is 160 wt%.

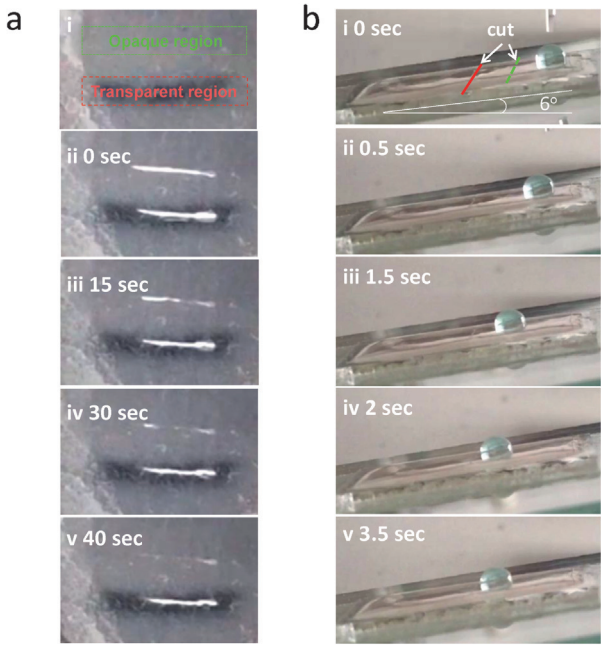

Figure 4. Localized recovery and the sliding of a water droplet on a patterned coating damaged by cutting with a knife. a) Optical images of the coating before damage (i) and after damage at 0 s (ii), 15 s (iii), 30 s (iv), and 40 s (v). b) Optical images of a water droplet (10 μL) on the damaged coating at 0 s (i), 0.5 s (ii), 1.5 s (iii), 2 s (iv), and 3.5 s (v). The solid and dashed lines indicate damage to the transparent and opaque regions, respectively.

expected to control this self-regulated secretion of the coatings. To demonstrate this capability, we compared the damage-induced secretion in different regions by manually inducing tentative damage with a knife (Figure 4a and Movie S3). The damage to the opaque region vanished soon whereas the cut in the transparent region remained, indicating that secretion is localization-dependent. This property could be used to control the motion of water droplets on the patterned coatings (Figure 4b and Movie S4). When both the covered and uncovered regions were subjected to linear damages, a water droplet could smoothly pass over the uncovered region but stuck to the covered region.

In conclusion, we have described a simple method to localize liquid droplets in polymer matrices that are directly formed from their precursor solution by evaporative lithography. Patterned compositions and phases were produced with this method. When the solvent evaporates selectively under a mask, liquid and polymer in a homogeneous state are redistributed. The polymer responsible for the resulting cross-linked matrices moves to the region of hindered evaporation while the excess nonvolatile liquid concentrates in the region with faster evaporation, triggering the phase separation to create liquid droplets. After gelation, droplet-containing and droplet-free regions display distinct properties. The general principle demonstrated with a simple three-composition system can be applied to different material systems for localizing material functions such as slipperiness, self-healing, and fouling resistance.

Experimental Section

A uPDMS solution (300 μL) and silicone oil in THF were coated onto a $1.5 \times 2.5\ cm^2$ glass substrate with a pipette. The system was immediately covered with a home-made Al mask and then left to dry in air for 24 h before characterization. Films with a thickness of 320 ± 20 μm were obtained.

Acknowledgements

J.C. acknowledges support from the Leibniz Research Cluster (419313).

Keywords: dynamic materials · evaporative lithography · liquid droplets · polymer matrices · supramolecular gels

How to cite: *Angew. Chem. Int. Ed.* **2016**, *55*, 10681–10685
Angew. Chem. **2016**, *128*, 10839–10843

[1] a) A. P. Esser-Kahn, S. A. Odom, N. R. Sottos, S. R. White, J. S. Moore, *Macromolecules* **2011**, *44*, 5539 – 5553; b) L. J. De Cock, S. De Koker, B. G. De Geest, J. Grooten, C. Vervaet, J. P. Remon, G. B. Sukhorukov, M. N. Antipina, *Angew. Chem. Int. Ed.* **2010**, *49*, 6954 – 6973; *Angew. Chem.* **2010**, *122*, 7108 – 7127; c) M. Humar, M. Ravnik, S. Pajk, I. Musevic, *Nat. Photonics* **2009**, *3*, 595 – 600.

[2] B. J. Blaiszik, S. L. B. Kramer, S. C. Olugebefola, J. S. Moore, N. R. Sottos, S. R. White, *Annu. Rev. Mater. Res.* **2010**, *40*, 179 – 211.

[3] a) H. Kikuchi, M. Yokota, Y. Hisakado, H. Yang, T. Kajiyama, *Nat. Mater.* **2002**, *1*, 64 – 68; b) V. Vorflusev, S. Kumar, *Science* **1999**, *283*, 1903 – 1905; c) X. Jia, J. Mei, J. Lai, C. Li, X. You, *Chem. Commun.* **2015**, *51*, 8928 – 8930.

[4] a) D. Quéré, *Rep. Prog. Phys.* **2005**, *68*, 2495 – 2532; b) J. Cui, D. Daniel, A. Grinthal, K. Lin, J. Aizenberg, *Nat. Mater.* **2015**, *14*, 790 – 795; c) Y. Li, L. Li, J. Sun, *Angew. Chem. Int. Ed.* **2010**, *49*, 6129 – 6133; *Angew. Chem.* **2010**, *122*, 6265 – 6269; d) C. Urata, G. J. Dunderdale, M. W. England, A. Hozumi, *J. Mater. Chem. A* **2015**, *3*, 12626 – 12630; e) T. S. Wong, S. H. Kang, S. K. Y. Tang, E. J. Smythe, B. D. Hatton, A. Grinthal, J. Aizenberg, *Nature* **2011**, *477*, 443 – 447; f) S. Anand, A. T. Paxson, R. Dhiman, J. D. Smith, K. K. Varanasi, *ACS Nano* **2012**, *6*, 10122 – 10129.

[5] a) R. W. Style, R. Boltyanskiy, B. Allen, K. E. Jensen, H. P. Foote, J. S. Wettlaufer, E. R. Dufresne, *Nat. Phys.* **2015**, *11*, 82 – 87; b) S. C. Ligon-Auer, M. Schwentenwein, C. Gorsche, J. Stampfl, R. Liska, *Polym. Chem.* **2016**, *7*, 257 – 286.

[6] a) S. R. White, N. R. Sottos, P. H. Geubelle, J. S. Moore, M. R. Kessler, S. R. Sriram, E. N. Brown, S. Viswanathan, *Nature* **2001**, *409*, 794 – 797; b) B. G. Trewyn, I. I. Slowing, S. Giri, H.-T. Chen, V. S. Y. Lin, *Acc. Chem. Res.* **2007**, *40*, 846 – 853; c) L. Wang, Z. Zhang, Y. Ding, *Soft Matter* **2013**, *9*, 4455 – 4463; d) Y. Luo, K. Cheng, N. Huang, W. Chiang, S. Li, *J. Polym. Sci. Part B* **2011**, *49*, 1022 – 1030; e) W. Wang, M. Zhang, L. Chu, *Acc. Chem. Res.* **2014**, *47*, 373 – 384.

[7] a) C. M. Jewell, D. M. Lynn, *Adv. Drug Delivery Rev.* **2008**, *60*, 979 – 999; b) D. Tian, Y. Song, L. Jiang, *Chem. Soc. Rev.* **2013**, *42*, 5184 – 5209; c) N. Vogel, R. A. Belisle, B. Hatton, T.-S. Wong, J. Aizenberg, *Nat. Commun.* **2013**, *4*, 3176; d) U. H. F. Bunz, *Adv. Mater.* **2006**, *18*, 973 – 989; e) D. Beysens, C. M. Knobler, *Phys. Rev. Lett.* **1986**, *57*, 1433 – 1436; f) A. Zhang, H. Bai, L. Li, *Chem. Rev.* **2015**, *115*, 9801 – 9868.

[8] a) N. Vogel, M. Retsch, C. Fustin, A. del Campo, U. Jonas, *Chem. Rev.* **2015**, *115*, 6265 – 6311; b) X. Tang, S. J. O'Shea, I. U. Vakarelski, *Adv. Mater.* **2010**, *22*, 5150 – 5153; c) D. J. Harris, H. Hu, J. C. Conrad, J. A. Lewis, *Phys. Rev. Lett.* **2007**, *98*, 148301; d) A. Georgiadis, A. F. Routh, M. W. Murray, J. L. Keddie, *Soft Matter* **2011**, *7*, 11098 – 11102; e) I. U. Vakarelski, D. Y. C. Chan, T. Nonoguchi, H. Shinto, K. Higashitani, *Phys. Rev. Lett.* **2009**, *102*, 058303.

[9] R. D. Deegan, O. Bakajin, T. F. Dupont, G. Huber, S. R. Nagel, T. A. Witten, *Nature* **1997**, *389*, 827 – 829.

[10] A. Utgenannt, J. L. Keddie, O. L. Muskens, A. G. Kanaras, *Chem. Commun.* **2013**, *49*, 4253 – 4255.

[11] a) N. J. Cira, A. Benusiglio, M. Prakash, *Nature* **2015**, *519*, 446 – 450; b) H.-J. Butt, D. S. Golovko, E. Bonaccurso, *J. Phys. Chem. B* **2007**, *111*, 5277 – 5283; c) H. Hu, R. G. Larson, *Langmuir* **2005**, *21*, 3972 – 3980.

[12] Estimated by the absorption intensity of dyed silicone oil. The real value should be higher as PDI-conjugated silicone oil has a lower mobility than normal silicone oil. The swelling ratio of silicone oil to uPDMS-Me is 98 wt% (oil/uPDMS-Me), and a coating with a silicone oil loading of 100 wt% would be opaque. Therefore, the loading of silicone oil in the transparent region was expected to be lower than 98 wt%. The total loading of silicone oil in the film was 160 wt%. Based on the assumption that the silicone oil did not evaporate, the loading of silicone oil in the opaque region should be higher than 160 wt%, which results in a silicone/oil loading ratio of > 1.63.

[13] a) F. Schellenberger, J. Xie, N. Encinas, A. Hardy, M. Klapper, P. Papadopoulos, H.-J. Butt, D. Vollmer, *Soft Matter* **2015**, *11*, 7617 – 7626; b) X. Deng, L. Mammen, Y. Zhao, P. Lellig, K. Müllen, C. Li, H.-J. Butt, D. Vollmer, *Adv. Mater.* **2011**, *23*, 2962 – 2965.

Received: May 18, 2016
Revised: June 16, 2016
Published online: July 27, 2016

